ARCH. MECH. TECH. MATER.VOL. 39, (2019) 16-25

DE GRUYTER OPEN

ARCHIVES OF MECHANICAL TECHNOLOGY AND MATERIALS
WWW.AMTM.PUT.POZNAN.PL

Kinematic model of multiple trailers on a tractor system for production logistics applications

Wojciech Paszkowiak[a], Tomasz Bartkowiak[a]*, Marcin Pelic[a]

[a]*Poznan University of Technology, Institute of Mechanical Technology, Pl. M. Sklodowskiej-Curie 5, 60-965 Poznan, Poland*

[*] *Corresponding author,tomasz.bartkowiak@put.poznan.pl*

ARTICLE INFO

Received 24 January 2019
Received in revised form 26 March 2019
Accepted 26 July 2019

KEY WORDS

Milk-runner
Kinematic analysis
Steering system
Collision
Validation

ABSTRACT

This paper demonstrates kinematic analysis of multiple trailers on a tractor system for production logistics. The analysis concerned three different steering systems of the trailers: virtual clutch and drawbar system, conventional clutch and drawbar system, double Ackermann steering system. Designed kinematic models contain various variants of paths: turning at a constant value of the steering angle, changing the steering angle as a result of an approaching collision. Each of these variants also included driving in a straight line after a 90° turn. The validation of the developed kinematic model was done by using a real logistic train, which path was registered via aerial drone. For each of the developed kinematic models, a visualization of drive through the 90° turn was created.

1. INTRODUCTION

The objective of this paper is to develop a credible kinematic model of a multiple trailer on a truck system for the most popular production logistics applications including the most common steering: virtual clutch and drawbar system, conventional clutch and drawbar system as well as double Ackermann steering. This model should contribute to a better understanding of an impact of geometrical relations on the trajectory of that system in motion. This can facilitate the trailer design for improved maneuverability in narrow corridors. The additional aim of this work was to validate the kinematic model by comparing calculated and actual trajectories of trailers while turning. The presented iterative kinematic model allows to calculate the locations of the tractor and towed trailers without taking into accounts the dynamics of the entire system.

1.1. Milk-runner

Milk-runner allows delivery and collection from multiple workstations with a single supplier. An intralogistics train with a platform system supplies the materials and components required for production. As a result, the vacant space in the transport system can be used to collect waste and spare material from the workplace. This allows a significant reduction in the number of rides [15].
A logistic train consisting of a tractor and a certain number of trailers or trolleys is a means of transport used within production plants and warehouses. It has been developed to increase the efficiency of transport within the company. In traditional systems, in which inter-operational transport using forklifts becomes inefficient for repeated path sequences, the rationality of using forklifts for purely transport purposes decreases in a direct proportion to the number of operated stations and the area of the warehouse or production hall. The implementation of a logistics train allows:

DOI: 10.2478/amtm-2019-0004

- increased efficiency,
- improved economy,
- flexibility,
- versatility,
- improved safety [12,13,14].

1.2. *Steering system*

A growing interest in intralogistics transportation has led to the development of new solutions. The main tendency here is to improve the efficiency by increasing the volume of transported goods. This can be achieved by using a larger number of trolleys. The transportation capacity can be increased using passive trailers, while the cost of the vehicle with trailers is much lower than the cost of multiple self-driven vehicles [4]. On the other hand, the larger number of trolleys can lead to difficulties in maintaining the desired path, especially in narrow spaces. The control of such multi-body systems becomes more complex due to complicated equations of motion, higher number of nonholonomic constraints, nonlinearities, potential collisions, skidding or jackknife effect [1].

The classic solution for connecting the trolleys using the drawbar at the front of the unit proved to be insufficient [9]. It has become a reason to look for new solutions in the field of steering systems of logistics trolleys that enable a specific route to be covered by a tractor with more units and optimization of train parameters. Applied steering systems in intralogistics differ significantly in their characteristics and capabilities[13].

1.3. *Drawbar system in a wheeled mobile robot*

The virtual clutch and conventional clutch with drawbar system are also used in other fields. These systems have found application in wheeled mobile robots (WMRs)[6]. Due to the complexity of system dynamics, the mathematical models of mobile robots have some simplifications [4].

Rouchon et al. presented a solution of the motion planning without obstacles for the nonholonomic system describing a car with n trailers. This solution relies on the fact that the system is flat with the cartesian coordinates of the last trailer as linearizing output [9].

Carrying out a kinematic analysis for mobile robots involves the same procedure as for logistic trolleys. In the analysis, the robot is treated as a rigid body ignoring the connections and internal degrees of freedom of the robot and its wheels. In order to determine the location of the robot on the reference plane, the relationships between the global coordinate system and the local robot coordinate system is established (Fig.1.). It is necessary to specify a reference point, which locates the origin of the local coordinate system of the unit. The position of the robot in the reference coordinate system is to define the location of point B_0 and angle β_0 between the axis of the reference and local coordinate systems by means of coordinates [10].

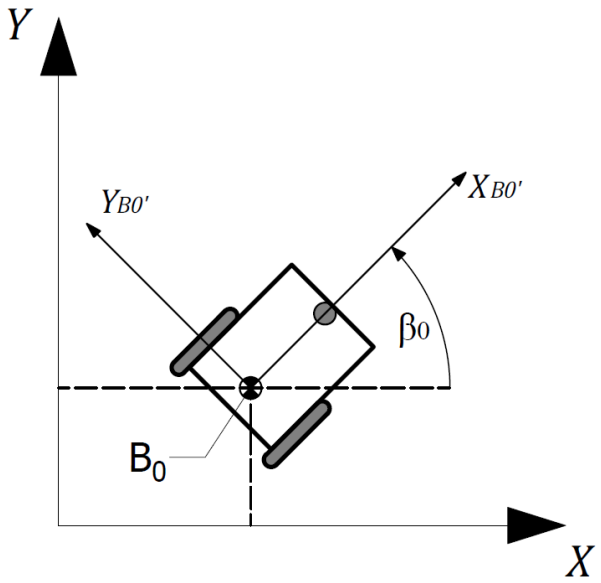

Fig. 1. The global coordinate system {X, Y} and the robot local coordinate system {XB0′, YB0′} [10]

It is necessary to map the described movement of the robot with reference components movements. Mapping is done using an orthogonal rotation matrix:

$$\mathbf{R}(\beta_0) = \begin{bmatrix} \cos\beta_0 & \sin\beta_0 & 0 \\ -\sin\beta_0 & \cos\beta_0 & 0 \\ 0 & 0 & 1 \end{bmatrix} [10]. \qquad (1)$$

1.4. *Tractor - trailer systems*

The most common mathematical models of the tractor towing a trailer are dynamic models with nonholonomic constraints. The constraints define strictly the movement path of the units of the systems. The dynamic equation of nonholonomic system is derived by the Lagrange formula. The Jacobian matrix describes the kinematic part of the model. The relation between the Jacobian matrix and system constraint matrix enables the model to reduce. Then the trajectory is defined by two kinematic inputs and the Jacobian matrix [2, 3, 5, 7, 11].

This paper proposes iterative kinematic model for tractor – trailer systems. Dynamics is not included in this model. It is easier to define a specific trajectory of the tractor as an input parameter.

2. KINEMATIC ANALYSIS

The presented kinematic analysis includes the kinematic model of the tractor, the kinematic model of the drawbar system, the kinematic model for the double Ackermann system, the algorithm detecting the approaching collision and the visualization of the train drive [8]. The calculation procedure is carried out iteratively. The results obtained in the previous iteration are necessary for the next step.

2.1. Tractor with Ackermann steering system

The main reference point of the tractor is point B_0.The parameter describing the turn of the tractor is the steering angle of the virtual wheel α_{0s}or, in short, steering angle (Fig. 2.).

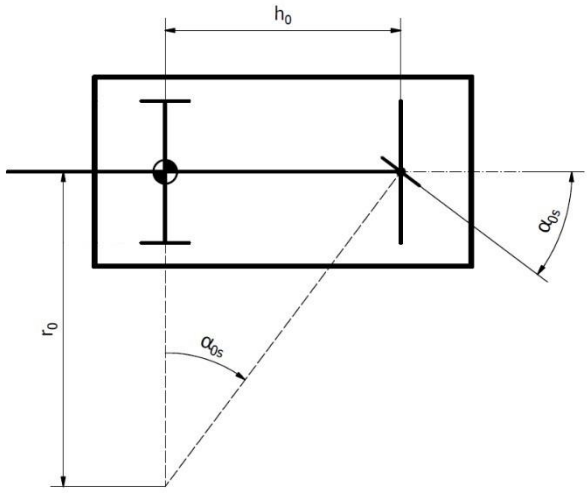

Fig. 2. The steering angle of the tractor's virtual wheel

The steering radius of the tractor is expressed as

$$r_0 = \frac{h_0}{\tan(\alpha_{0s})}. \tag{2}$$

2.1.1. Constant value of the steering angle

The steering angle of the virtual wheel α_{0s} and angle $\beta_0$describing the arc length of the covered path by point B_0 are two main parameters describing the character of the road covered by the tractor (Fig. 3).

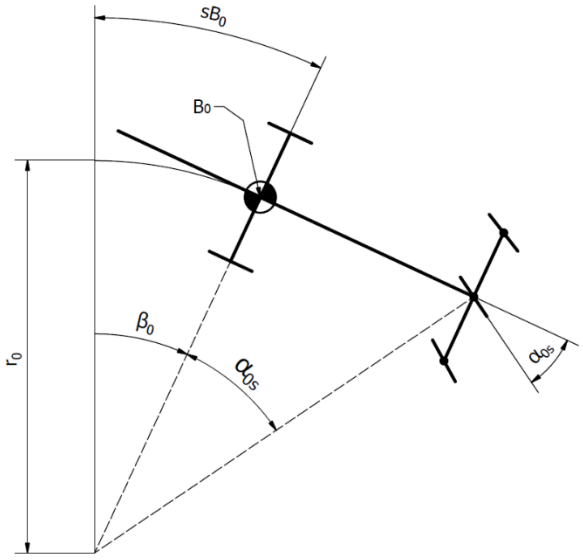

Fig. 3. Change of tractor position

In order to clearly define the location of tractor points, the initial position of the point B_0 was described by the parameters x and y. They determine the position of the tractor main point relative to the start of the fixed coordinate system (Fig. 4).

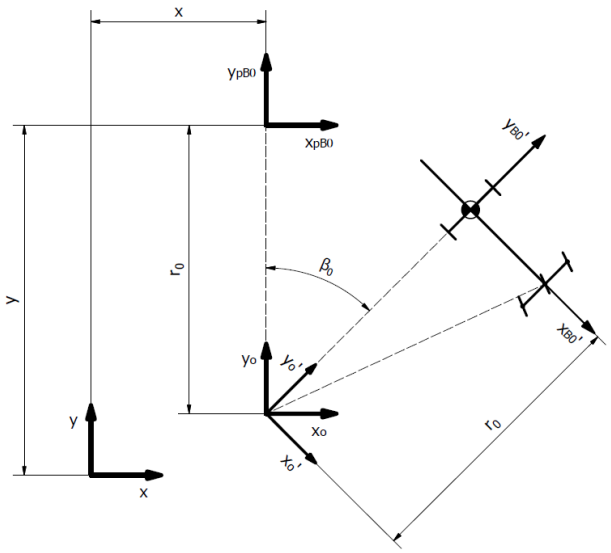

Fig. 4. Position of the tractor relative to the main coordinate system {x, y}

The angle rotation matrix β_0 for *i-th* iteration is described as

$$\mathbf{R}(-\beta_0\, i) = \begin{bmatrix} \cos(i\,\beta_0) & \sin(i\,\beta_0) \\ -\sin(i\,\beta_0) & \cos(i\,\beta_0) \end{bmatrix}, \tag{3}$$

where i is the iteration number. The position of point B_0 to the origin of the coordinate system after rotation is described by the expression:

$$\mathbf{B_{0xy}} = \mathbf{R}(-\beta_0\, i)\left[\mathbf{B_{0xyf}} + \begin{bmatrix} 0 \\ r_0 \end{bmatrix}\right] - \begin{bmatrix} 0 \\ r_0 \end{bmatrix} + \begin{bmatrix} x \\ y \end{bmatrix}, \tag{4}$$

where $\mathbf{B_{0xyf}}$is the coordinate of point B_0 in the local coordinate system of the tractor. The position of any tractor point in the main coordinate system is defined as

$$\mathbf{xy_0} = \mathbf{R}(-\beta_0\, i)\left[\mathbf{xyf_0} + \begin{bmatrix} 0 \\ r_0 \end{bmatrix}\right] - \begin{bmatrix} 0 \\ r_0 \end{bmatrix} + \begin{bmatrix} x \\ y \end{bmatrix}, \tag{5}$$

where $\mathbf{xyf_0}$are coordinates of the selected point in the local coordinate system of the tractor.

2.1.2. Changing the steering angle

For tractor motion with changing steering angle value, it is important to keep constant accuracy. In order to obtain constant accuracy in each iteration, a constant point A_0 displacement is necessary for each step (Fig. 5).

The value of the distance travelled by point A_0 during one iteration is expressed as

$$dL = \Big((r_0\sin(\beta_{0I}) + h_0\cos(\beta_{0I}) - h_0)^2 + \big(r_0 - (r_0\cos(\beta_{0I}) - h_0\sin(\beta_{0I}))\big)^2\Big)^{\frac{1}{2}}, \quad (6)$$

where β_{0I} is the rotation angle in one step for the calculation procedure ensuring constant accuracy.

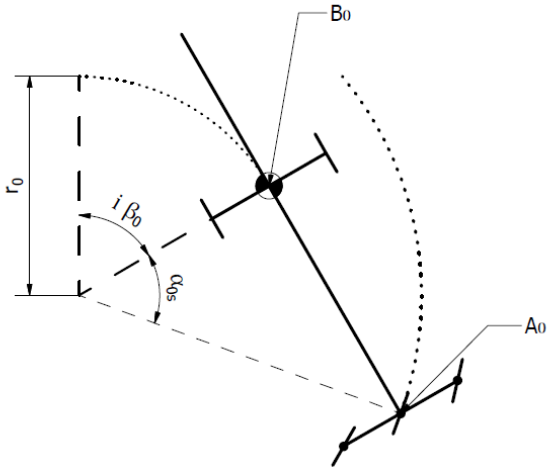

Fig. 5. Movement of point A_0

The value of the tractor's rotation angle during one iteration needed to maintain constant accuracy is

$$\beta_{2I} = \arccos\Big(-\frac{1}{4}\big(2\cos(2\,\alpha_{1s}) - 2\cos(2\,\alpha_{2s}) + \cos(2\,\alpha_{2s} - \beta_{1I}) - 2\cos(\beta_{1I}) + \cos(2\,\alpha_{2s} + \beta_{1I})\big)\csc(\alpha_{1s})^2\Big), \quad (7)$$

where:
α_{1s} – the previous value of angle α_{0s},
α_{2s} – the new value of angleα_{0s},
β_{1I} – the previous value of angle β_{0I}.

The change in the steering angle determines the change in the steering radius value. This affects the change of the origin position of the coordinate system $\{x_o, y_o\}$. Figure 6 illustrates the effect of changing the value of the steering angle on the location of the aforementioned coordinate system.
On that basis, new parameters R_{xN} and R_{yN} have been introduced, taking into account the displacement of the coordinate system $\{x_o, y_o\}$. The position of point B_0 with a changing steering angle is expressed by

$$\mathbf{B_{0xy}} = \mathbf{R}(-\beta_{0C})\left[\mathbf{B_{0xyf}} + \begin{bmatrix}0\\ r_0\end{bmatrix}\right] + \begin{bmatrix}R_{xN}\\ R_{yN}\end{bmatrix} + \begin{bmatrix}x\\ y\end{bmatrix}. \quad (8)$$

where
$\beta_{0C} = \beta_{0C} + \beta_{0I}$ and $\beta_{0C} = 0$ for $i = 1$,
$R_{xN} = x_{B0} - r_0\sin(\beta_{0C}) - x$ and$R_{xN} = 0$ for $i = 1$,
$R_{yN} = y_{B0} - r_0\cos(\beta_{0C}) - y$ and$R_{yN} = -r_0$for $i = 1$,

x_{B0}, y_{B0} – mean the coordinates of the position of pointB_0.

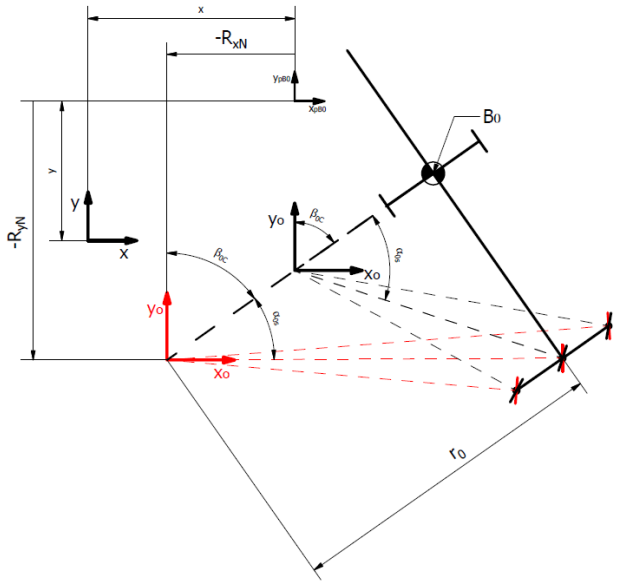

Fig. 6. Changing value of the steering angle

The position of any tractor point in the main coordinate system is defined as

$$\mathbf{xy_0} = \mathbf{R}(-\beta_{0c})\left[\mathbf{xyf_0} + \begin{bmatrix}0\\ r_0\end{bmatrix}\right] + \begin{bmatrix}R_{xN}\\ R_{yN}\end{bmatrix} + \begin{bmatrix}x\\ y\end{bmatrix}. \quad (9)$$

2.1.3. Driving in a straight line

After90° turn, the tractor travels in a straight line. The parameter L_p, describing the travelled distance, has been entered. $L_p = 0$ for $i = 1$. In other cases

$$L_p = L_p + dL\,. \quad (10)$$

The position of the point of any tractor point when moving in a straight line for the constant steering angle version is

$$\mathbf{xy_0} = \mathbf{R}(-\beta_0\, i)\left[\mathbf{xyf_0} + \begin{bmatrix}L_p\\ r_0\end{bmatrix}\right] - \begin{bmatrix}0\\ r_0\end{bmatrix} + \begin{bmatrix}x\\ y\end{bmatrix}, \quad (11)$$

for the changing steering angle version is

$$\mathbf{xy_0} = \mathbf{R}(-\beta_{0C})\left[\mathbf{xyf_0} + \begin{bmatrix}L_p\\ r_0\end{bmatrix}\right] + \begin{bmatrix}R_{xN}\\ R_{yN}\end{bmatrix} + \begin{bmatrix}x\\ y\end{bmatrix}. \quad (12)$$

2.2. Virtual clutch and conventional clutch with drawbar system

The calculation procedure for virtual clutch and conventional clutch is identical. The index k is the number of the trolley. The geometrical parameters of the trolley are shown in Figure 7.

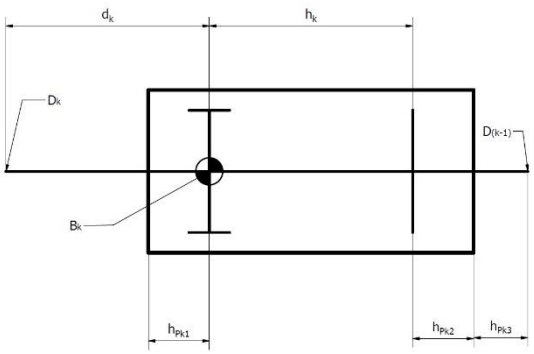

Fig. 7. Trolley parameters for virtual clutch and conventional clutch

2.2.1. Kinematic model

The kinematic procedure was divided into several stages. Knowing the current position of the trolley and the new location of the tractor, rotation relative to point B_1 is performed in such a way that the trolley axis intersects the point D_0 (Fig. 8).

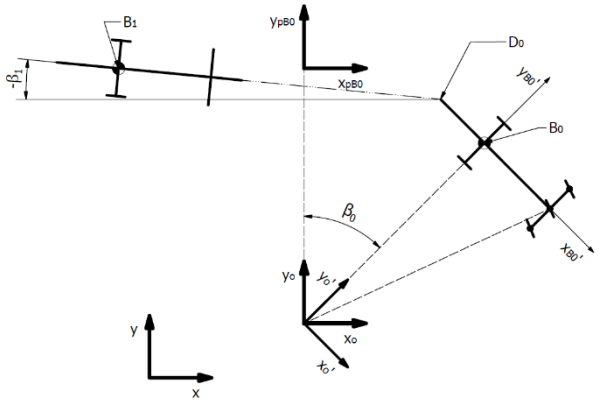

Fig. 8. Rotation of the first trolley relative to point B_1

Based on Figure 8, the inclination angle of the trolley in relation to the horizontal line of the main coordinate system was determined as

$$\beta_1 = \operatorname{arctg}\left(\frac{y_{B0} - y_{B1} + d_0 \sin(\beta_0\, i)}{x_{D0} - x_{B1}}\right), \tag{13}$$

where:
x_{B1}, y_{B1} – the coordinate of point B_1,
x_{D0} – the coordinate of point D_0,
y_{B0} – the coordinate of point B_0.

The angle between the axes of the tractor and the first trolley is denoted as

$$\gamma_1 = \beta_0\, i + \beta_1\,. \tag{14}$$

The rotation matrix of the *k-th* trolley is denoted as

$$\mathbf{R}(\gamma_k) = \begin{bmatrix} \cos\gamma_k & -\sin\gamma_k \\ \sin\gamma_k & \cos\gamma_k \end{bmatrix}. \tag{15}$$

After rotation, the trolley moves along its axis in such a way that a connection between units is created (Fig. 9.).

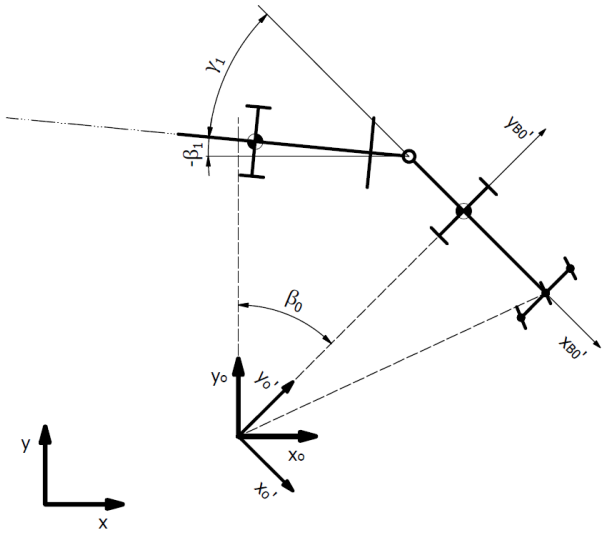

Fig. 9. Moving the trolley along its axis

Taking into account the above expressions, the location of any point of the first trolley in the main coordinate system is denoted as

$$\mathbf{xy_1} = \mathbf{R}(-\beta_0\, i)\left[\mathbf{R}(\boldsymbol{\gamma_1})\left[\mathbf{xyf_1} - \begin{bmatrix} h_1 + h_{P12} + h_{P13} \\ 0 \end{bmatrix}\right] - \begin{bmatrix} d_0 \\ 0 \end{bmatrix} + \begin{bmatrix} 0 \\ r_0 \end{bmatrix}\right] - \begin{bmatrix} 0 \\ r_0 \end{bmatrix} + \begin{bmatrix} x \\ y \end{bmatrix}, \tag{16}$$

where $\mathbf{xyf_1}$ are coordinates of the selected point in the local coordinate system of the first trolley.

For the next trolleys, the calculation is done in the same way. The angles describing the rotation of the *k-th* trolley are denoted as

$$\beta_k = \operatorname{arctg}\left(\frac{-y_{B(k-1)} + y_{Bk} + d_{(k-1)}\sin(\beta_{k-1})}{x_{Bk} - x_{D(k-1)}}\right), \tag{17}$$

$$\gamma_k = \beta_k - \beta_{k-1}\,. \tag{18}$$

The location of the selected *k-th* point of the trolley relative to the trolley *k-1* is denoted as

$$\mathbf{xyf}_{\mathbf{kx_{B(k-1)'}y_{B(k-1)'}}} = \mathbf{R}(\gamma_k)\left[\mathbf{xyf}_{\mathbf{(k+1)x_{Bk'}y_{Bk'}}} - \begin{bmatrix} h_k + h_{Pk2} + h_{Pk3} \\ 0 \end{bmatrix}\right] - \begin{bmatrix} d_{k-1} \\ 0 \end{bmatrix}, \tag{19}$$

The location of the *k-th* point of the trolley in the main coordinate system $\{x, y\}$:

- for the constant steering angle version is

$$\mathbf{xy_k} = \mathbf{R}(-\beta_0\, i)\left[\mathbf{xyf_{kx_{B0'}y_{B0'}}} + \begin{bmatrix}0\\ r_0\end{bmatrix}\right] - \begin{bmatrix}0\\ r_0\end{bmatrix} + \begin{bmatrix}x\\ y\end{bmatrix}, \qquad (20)$$

- for the changing steering angle version is

$$\mathbf{xy_k} = \mathbf{R}(-\beta_{0C})\left[\mathbf{xyf_{kx_{B0'}y_{B0'}}} + \begin{bmatrix}0\\ r_0\end{bmatrix}\right] + \begin{bmatrix}R_{xN}\\ R_{yN}\end{bmatrix} + \begin{bmatrix}x\\ y\end{bmatrix}, \qquad (21)$$

- for the driving in a straight line version is

$$\mathbf{xy_k} = \mathbf{R}(-\beta_{0C})\left[\mathbf{xyf_{kx_{B0'}y_{B0'}}} + \begin{bmatrix}L_p\\ r_0\end{bmatrix}\right] + \begin{bmatrix}R_{xN}\\ R_{yN}\end{bmatrix} + \begin{bmatrix}x\\ y\end{bmatrix}, \qquad (22)$$

2.3. Double Ackermann steering system

The double Ackermann system is significantly different from the two previous steering systems. In the kinematic model the rotary drawbar is attached to the front axle of the trolley. The geometrical parameters of the trolley are presented in Figure 10.

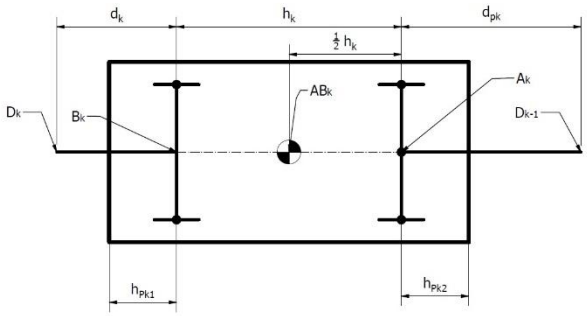

Fig. 10. Trolley parameters for double Ackermann steering system

2.3.1. Kinematic model

Due to the complex kinematics of the double Ackermann system, there are more stages for the calculation procedure than in the previous steering systems.

Knowing the current position of the drawbar and the new location of the tractor, the rotation relative to point A_1 is carried out in such a way that the extension of the drawbar intersects the point D_0 (Fig. 11).

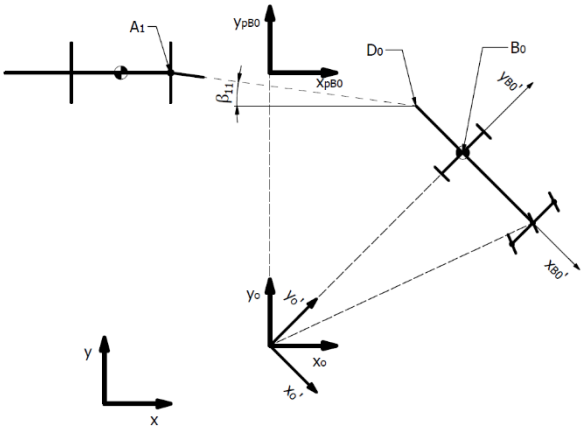

Fig. 11. Drawbar rotation relative to point A_1

The new position makes it possible to describe the angles defining the drawbar's orientation:

$$\beta_{k1} = \operatorname{arctg}\left(\frac{y_{Ak} - y_{D(k-1)}}{x_{D(k-1)} - x_{Ak}}\right), \qquad (23)$$

for $k = 1$:

$$\gamma_{11} = -\beta_{11} + \beta_0, \qquad (24)$$

for $k > 1$:

$$\gamma_{k1} = -\beta_{k1} + \beta_{(k-1)2}, \qquad (25)$$

where index k is the number of the trolley.

The rotation matrix for angle γ_{k1} for the *k-th* trolley is denoted as

$$\mathbf{R}(\gamma_{k1}) = \begin{bmatrix}\cos(\gamma_{k1}) & -\sin(\gamma_{k1})\\ \sin(\gamma_{k1}) & \cos(\gamma_{k1})\end{bmatrix}. \qquad (26)$$

After rotation, the drawbar moves along its axis. The trolley translates so that the connection between adjacent trolley and a tractor is maintained. (Fig. 12.).

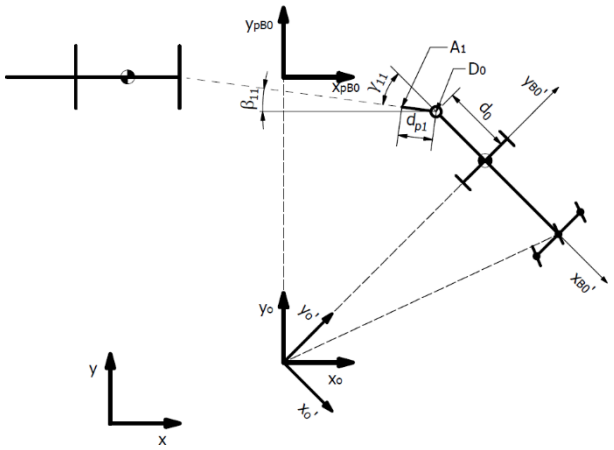

Fig. 12. The drawbar connects to the tractor

The displacement of the drawbar allows the determination of new coordinates of point A_1, for the *i-th* iteration it was denoted as

$$\mathbf{A_{1xy}} = \mathbf{R}(-\beta_0\, i)\left[\mathbf{A_{1x_{B0'}y_{B0'}}} + \begin{bmatrix}0\\ r_0\end{bmatrix}\right] - \begin{bmatrix}0\\ r_0\end{bmatrix} + \begin{bmatrix}x\\ y\end{bmatrix}. \qquad (27)$$

Knowing the new position of the drawbar, the rotation relative to point AB_1 is carried out in such a way that the extension of the trolley axis intersects point A_1 (Fig. 13).
The new position makes it possible to describe the angles defining the trolley orientation:

$$\beta_{k2} = \operatorname{arctg}\left(\frac{y_{ABk} - y_{Ak}}{x_{Ak} - x_{ABk}}\right), \qquad (28)$$

$$\gamma_{k2} = -\beta_{k2} + \beta_{k1}, \tag{29}$$

where index k is the number of the trolley.

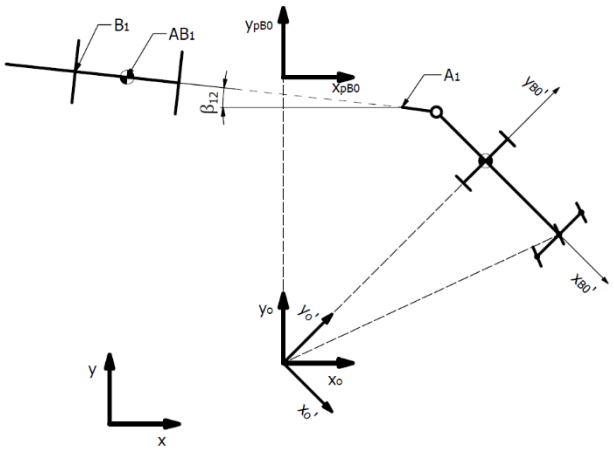

Fig. 13. Drawbar rotation relative to point A_1

The rotation matrix for angle γ_{k2} for the *k-th* trolley is denoted as

$$\mathbf{R}(\gamma_{k2}) = \begin{bmatrix} \cos\gamma_{k2} & -\sin\gamma_{k2} \\ \sin\gamma_{k2} & \cos\gamma_{k2} \end{bmatrix} \tag{30}$$

After rotation, the trolley moves along its axis in such a way that a connection between units is created (Fig. 14).

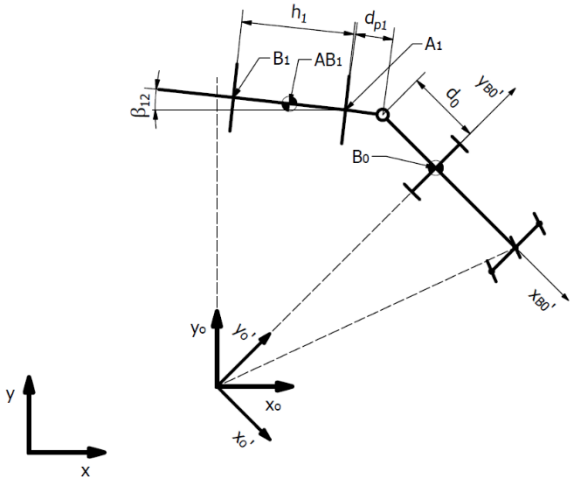

Fig. 14. The trolley connects to the drawbar

The location of the selected *k-th* point of the trolley relative to the trolley *k-1* is denoted as

$$\mathbf{xyf}_{\mathbf{kx_{B(k-1)'}y_{B(k-1)'}}} = \mathbf{R}(\gamma_{k1})\left[\mathbf{R}(\gamma_{k2})\left[\mathbf{xyf}_{\mathbf{(k+1)x_{Bk'}y_{Bk'}}} - \begin{bmatrix} h_k \\ 0 \end{bmatrix}\right] + \begin{bmatrix} -d_{pk} \\ 0 \end{bmatrix}\right] - \begin{bmatrix} d_{k-1} \\ 0 \end{bmatrix} \tag{31}$$

The location of the *k-th* point of the trolley in the main coordinate system $\{x, y\}$:

- for the constant steering angle version is

$$\mathbf{xy_k} = \mathbf{R}(-\beta_0\, i)\left[\mathbf{xyf}_{\mathbf{kx_{B0'}y_{B0'}}} + \begin{bmatrix} 0 \\ r_0 \end{bmatrix}\right] - \begin{bmatrix} 0 \\ r_0 \end{bmatrix} + \begin{bmatrix} x \\ y \end{bmatrix}. \tag{32}$$

- for the changing steering angle version is

$$\mathbf{xy_k} = \mathbf{R}(-\beta_{0C})\left[\mathbf{xyf}_{\mathbf{kx_{B0'}y_{B0'}}} + \begin{bmatrix} 0 \\ r_0 \end{bmatrix}\right] + \begin{bmatrix} R_{xN} \\ R_{yN} \end{bmatrix} + \begin{bmatrix} x \\ y \end{bmatrix}. \tag{33}$$

- for the driving in a straight line version is

$$\mathbf{xy_k} = \mathbf{R}(-\beta_{0C})\left[\mathbf{xyf}_{\mathbf{kx_{B0'}y_{B0'}}} + \begin{bmatrix} L_p \\ r_0 \end{bmatrix}\right] + \begin{bmatrix} R_{xN} \\ R_{yN} \end{bmatrix} + \begin{bmatrix} x \\ y \end{bmatrix}. \tag{34}$$

2.3.2. Steering angle of the wheels

The relation describing the angle γ_{k2} for the *k-th* trolley allows to define the steering angles of the wheels. The theoretical method assumes that the point relative to which the trolley rotates is exactly in the middle between the axes of the trolley (Fig. 15).

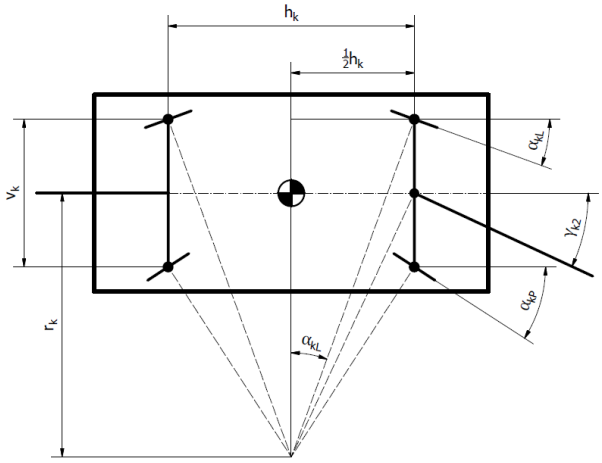

Fig. 15. Wheel steering in the double Ackermann system

The steering radius of the trolley is expressed as

$$r_k = \frac{\frac{1}{2}h1}{\tan(\gamma_{k2})}. \tag{35}$$

The steering angles are described as

$$\alpha_{kL} = \operatorname{arctg}\left(\frac{\frac{1}{2}h_k}{\left(r_k + \frac{1}{2}v_k\right)}\right), \tag{36}$$

$$\alpha_{kP} = \operatorname{arctg}\left(\frac{\frac{1}{2}h_k}{\left(r_k - \frac{1}{2}v_k\right)}\right). \tag{37}$$

2.4. Collision

A collision detection mechanism has been introduced to make a collision-free ride. Detection of an approaching

collision determines the change in the steering angle to a smaller one.

For virtual clutch and conventional clutch, the collision is detected using value between the trolleys (Fig. 16.).

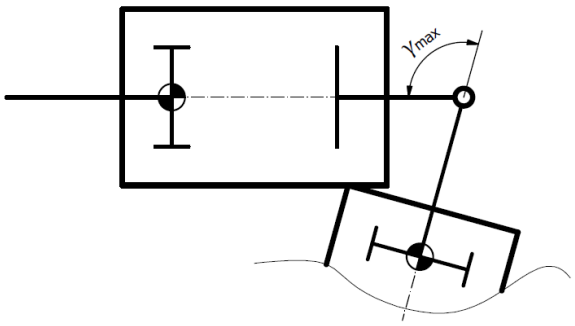

Fig. 16. Collision for the drawbar system

A collision is detected when the condition is fulfilled

$$\gamma_k > \gamma_{maxk} - \gamma_{tol}, \tag{38}$$

where γ_{tol} is a tolerance parameter that allows detection of a collision before it occurs.

For double Ackermann steering system, the collision is detected by means of a zone (Fig. 17.). The reason for changing the method of collision detection is the more complicated steering system.

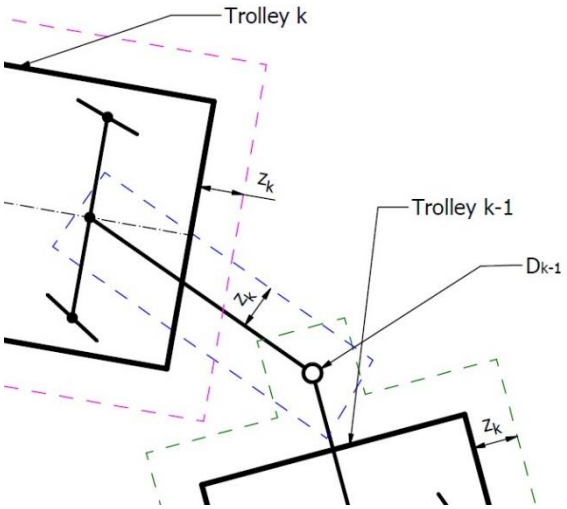

Fig. 17. Collision detection zones

A collision is detected when the extreme point of the trolley is in the zone of another trolley or in the drawbar area. The size of the zone is determined by the parameter z_k.

2.5. Visualization

The calculation procedure also allows visualization of the train drive. Figure 18 shows the comparison of trains with different steering systems.

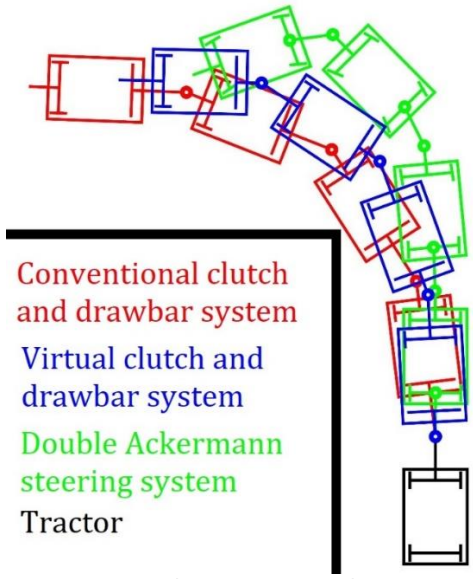

Fig. 18. Comparison of steering systems for constant valueα_{0s} = 70°along with driving in a straight line obtained by simulation

3. VALIDATION OF THE DRAWBAR SYSTEM

In order to verify the calculation procedure described in this article, the model validation process was carried out on the example of a real train. The test was carried out for the virtual clutch and drawbar system. The tractor was *Linde P30.*The validation was based on *ATRES INTRALOGISTICS platform trolley type H EURO.* The validation consisted of performing a curve ride with a constant value of the steering angle. The measurement was made by reading the location of reference points while the train is running. The location of the coordinate system is outside the frame of Figure19. Each unit has two reference points assigned (Fig. 19). We registered drive of a tractor towing three units using aerial drone fitted with HD digital camera. The locations of the reference points were obtained using image recognition software. The first two trailers were loaded to avoid the slip effect.

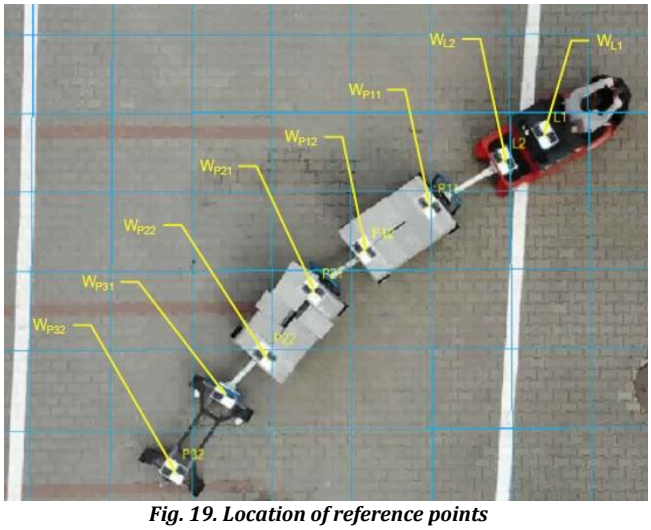

Fig. 19. Location of reference points

Figures 20 and 21 present a graphical comparison of the paths of two selected points for a relatively small value of the steering angle.

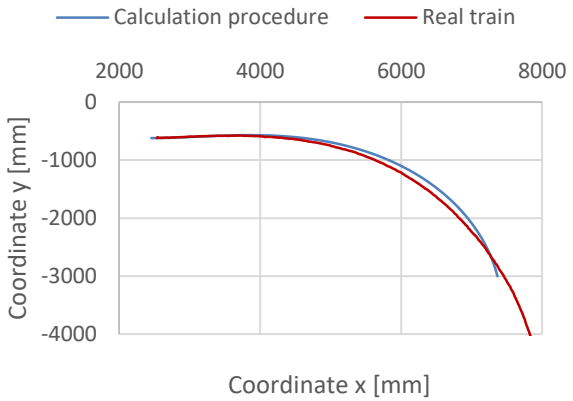

Fig. 20. Comparison of the W_{P12} for the steering angle $\alpha_{0s} = 17°$

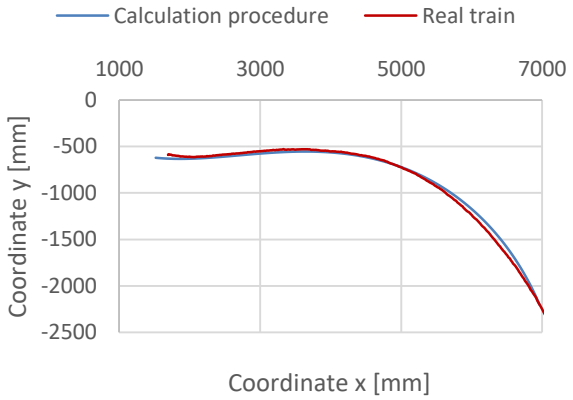

Fig. 21. Comparison of the W_{P21} for the steering angle $\alpha_{0s} = 17°$

The calculation procedure was carried out using the *Mathematica* environment. In this program, the final position of the train for driving with a steering angle of 17° was generated (Fig. 22.).

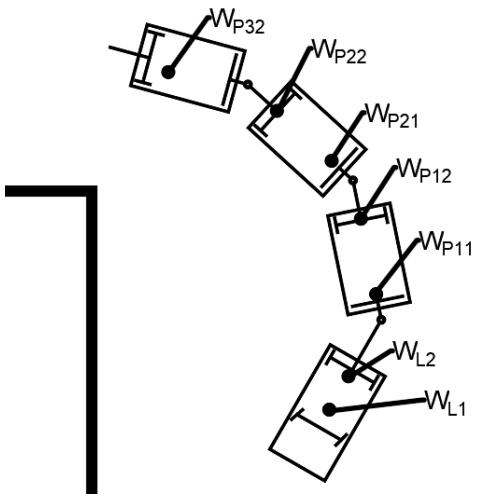

Fig. 22. The final position of the train for driving with a steering angle $\alpha_{0s} = 17°$, generated using the calculation procedure

Figures 23 and 24 present a comparison of the paths of the two previously mentioned points for almost the maximum value of the steering angle.

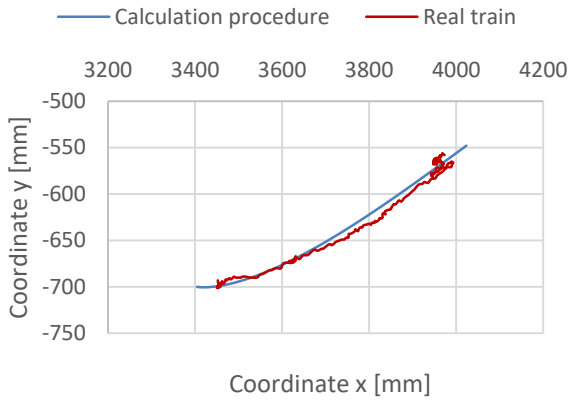

Fig. 23. Comparison of the W_{P12} for the steering angle $\alpha_{0s} = 80°$

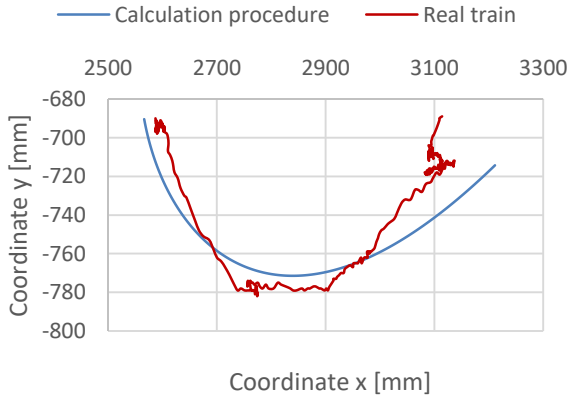

Fig. 24. Comparison of the W_{P21} for the steering angle $\alpha_{0s} = 80°$

4. CONCLUSIONS

The kinematic model of the logistic train allows conducting various types of analyzes, optimization procedures and graphically presenting the train running on a given route by means of animation. The mechanism enabling the detection of an approaching collision allows to reflect the actual driving in which the driver of the tractor reduces the turning angle in order to avoid the collision of units with each other. Collision detection allows checking the maneuverability of the entire system for given geometrical parameters of the logistic train.

Validation of the developed model of the kinematic system based on the example of a real train with a virtual clutch and drawbar system provided satisfactory results. The characteristics of the paths of the analyzed points are similar to the ones obtained using the calculation procedure. The value of the steering angle has a significant influence on the results. As the value of the steering angle increases, the convergence of results decreases. However, taking into account the testing conditions and resulting inaccuracies, we believe that the study was a success. It is probable that with greater accuracy of measurements, the obtained results may be almost identical to the results of the calculation

procedure. Differences in the obtained characteristics may result from:

- shifts of reference points. They were attached to concrete blocks that could move during the movement of the train.
- slip of individual trolleys.
- errors in the measurement method and image analyzing software.
- not taking into account angular limitations in joints.
- difficulties with recreating the driving conditions occurring during the simulation of the calculation procedure.

Comparing the analyzed steering systems it was found that for trains consisting of at least two trolleys, the virtual clutch and drawbar system or the double Ackermann system is the right choice. The double Ackermann system keeps the trajectory imposed by the tractor even with a large number of trolleys. The virtual clutch and drawbar system enables efficient drive through narrow and windy corridors.

REFERENCES

[1] **Altafini C.,**Some properties of the general n-trailer, Int J Control 2001; 74: 409–424.

[2] **Bravo-Doddoli A., Garcia-Naranjo L.,** The dynamics of an articulated n-trailer vehicle, Regular and Chaotic Dynamics, 20(5), pp.497-517, 2015.

[3] **Hou X., Yue M., Zhao J., Zhang X.,** An ESO-based integrated trajectory tracking control for tractor-trailer vehicles with various constraints and physical limitations, International Journal of Systems Science, 49(15), pp.3202-3215, 2018.

[4] **Keymasi Khalaji A., Moosavian S.A.A.,** Adaptive sliding mode control of a wheeled mobile robot towing a trailer,IMechE, 2014.

[5] **Keymasi Khalaji A., Moosavian S.A.A.,** Dynamic modeling and tracking control of a car with *n* trailers,Multibody System Dynamics 37(2), pp.211-225, 2015.

[6] **Keymasi Khalaji A., Moosavian S.A.A.,** Non-model based control for a wheeled mobile robot towing two trailers,IMechE, 2014.

[7] **Lashkari N., Biglarbegian M., Yang S.,** Backstepping Tracking Control Design for a Tractor Robot Pulling Multiple Trailers, Annual American Control Conference (ACC), 2018.

[8] **Paszkowiak W.,** Projekt układu kinematycznego pociągu logistycznego typu mleczarz i jego walidacja,Master Thesis, Poznan University of Technology, Poznań 2018.

[9] **Rouchon P., Fliess M., LE´ Vine J., et al.,** Flatness and motion planning: the car with n trailers, In: 2nd Europeancontrol conference, Groningen, NL, 28 June–1 July 1993,pp.1518–1522.

[10] **Siegwart R., Nourbakhsh I.,** Autonomous Mobile Robots, A Bradford Book, London 2004, pp 47-88.

[11] **Yue M., Hou X., Fan M., Jia R.,** Coordinated trajectory tracking control for an underactuated tractor-trailer vehicle via MPC and SMC approaches, 2017 2nd International Conference on Advanced Robotics and Mechatronics (ICARM), 2017.

[12] Internet portal dedicated to logistics (24.06.2018), available at: *www.logistyczny.com.*

[13] The official *ATRES INTRALOGISTICS* website (24.06.2018), available at: *www.atres.pl.*

[14] The official *LKE* website (24.06.2018), available at: *www.lke-intralogistik.com.*

[15] The official *WAMECH* website (24.06.2018), available at: *www.leanintralogistics.com.*